THE ASTROPHYSICAL JOURNAL, 323:306-315, 1987 December 1

PHOTOCHEMISTRY AND MOLECULAR IONS IN OXYGEN-RICH CIRCUMSTELLAR ENVELOPES

G. A. MAMON AND A. E. GLASSGOLD
Department of Physics, New York University

AND

A. OMONT
Groupe d'Astrophysique,[1] Observatoire de Grenoble, Université Scientifique et Médicale de Grenoble
Received 1987 March 9; accepted 1987 May 18

ABSTRACT

A theory for the ionization of the circumstellar envelopes around O-rich red giants is developed from the photochemical model. The main source of ionization is photoionization of H_2O, OH, and C by the interstellar UV radiation field, supplemented by cosmic-ray ionization of hydrogen. Significant amounts of H_3O^+ and HCO^+ are produced, with peak abundances $\sim 10^{-7}$ at intermediate distances from the star. Although H_3O^+ may be difficult to detect with current instrumentation, HCO^+ is probably detectable in nearby O-rich envelopes with large millimeter-wave telescopes.

Subject headings: molecular processes — stars: circumstellar shells — stars: late-type

I. INTRODUCTION

The study of the extended circumstellar envelopes (CSEs) of red giant stars can provide significant information on the late stages of stellar evolution and the chemical reprocessing of the interstellar medium. Basic to the subject is the understanding of the physical and chemical properties of these envelopes. Some of the earliest chemical information was obtained from the detection of infrared spectral features characteristic of dust formation in O-rich and C-rich environments. More recently, the potential for understanding the gas phase chemistry of circumstellar envelopes has been amply demonstrated by the detection of numerous molecules at radio wavelengths. For recent reviews of circumstellar chemistry, see Omont (1985) and Glassgold and Huggins (1986*a*).

Most attention has been focused on the nearby C-rich envelope, IRC +10216, which displays a rich hydrocarbon chemistry. With the help of large new millimeter-wave telescopes and arrays, other C-rich envelopes are now being investigated in detail. The observational study of O-rich CSEs is less well advanced, in part because CO tends to take up all the available gas phase carbon. O-rich envelopes do host astrophysically important OH, H_2O, and SiO masers (e.g., Walmsley 1987). Recent observations suggest that O-rich CSEs have an interesting chemical activity of their own. For example, HCN, SO_2, and SO have now been detected in several cases (Deguchi and Goldsmith 1985; Lucas *et al.* 1986; Guilloteau *et al.* 1986; Nercessian *et al.* 1987) and many molecules have been detected in the bipolar nebula OH 231.8+4.2 (Morris *et al.* 1987). In this paper, we present the first results of our research on the circumstellar chemistry of O-rich CSEs based on the photochemical model.

This model was introduced by Goldreich and Scoville (1976, henceforth GS) to explain the formation of OH masers in terms of the photoproduction of OH from H_2O The model was extended by Scalo and Slavsky (1980, also Slavsky and Scalo 1984) to include S and Si chemistry. Deguchi (1982) and Huggins and Glassgold (1982*a*) refined the GS treatment of photodissociation, and the latter authors showed that the correlation of OH maser position with mass loss rate (Bowers, Johnston, and Spencer 1981) could be interpreted in terms of a dust and H_2O self-shielding of the interstellar radiation field. The photochemical model has also been extensively applied to C-rich CSEs (Huggins and Glassgold 1982*b*, and the reviews by Omont 1985 and Glassgold and Huggins 1986*a*).

We have recently developed a theory of ionization of C-rich CSEs in which atomic and molecular ions produced by cosmic rays and penetrating UV radiation generate a rich ion-molecule chemistry in these envelopes (Glassgold, Lucas, and Omont 1986, hereafter Paper I; Glassgold *et al.* 1987, hereafter Paper II; see also Nejad, Millar, and Freeman 1984). Here, we extend the theory to O-rich CSEs and lay the foundations for a more comprehensive treatment of the chemistry of these envelopes. We restrict our considerations to the photochains associated with the most abundant heavy molecules, CO, H_2O, and N_2, which account for the bulk of the ionization. We also consider the possibilities for detecting particular molecular ions in order to obtain direct confirmation of the theory. In § II, we briefly introduce the photochemical model, emphasizing those features which distinguish O-rich and C-rich chemistry. The results of model calculations and the observability of HCO^+ and H_3O^+ are discussed in § III. A summary is given in § IV.

II. IONIZATION MODEL

a) Physical Basis

According to the photochemical model, interstellar UV radiation penetrates the CSE and dissociates and ionizes the neutral expanding wind. Cosmic rays provide a supplementary source of ionization in the form of hydrogen ions. The ionization and dissociation products then generate an active chemistry in the outer envelope, primarily by ion-molecule reactions.

For purposes of simplicity, we consider a steady spherically symmetric wind with constant expansion velocity V and hydrogen mass-loss rate $\dot{M}$, so that the total hydrogen density

[1] Associated with CNRS UA 708.

TABLE 1

STANDARD PARAMETERS

Parameter	Value
Hydrogen mass loss rate ($\dot{M}$)	$10^{-5}\ M_\odot\ \mathrm{yr}^{-1}$
Expansion velocity (V)	15 km s^{-1}
Gas kinetic temperature [$T(r)$]	$550\ r_{15}{}^{-0.7}$ K
Initial abundances:[a]	
CO	4×10^{-4}
H_2O	3×10^{-4}
N_2	10^{-4}

[a] Relative to hydrogen nuclei; the abundance of atomic hydrogen is assumed to be zero.

varies as

$$n(r) = C/r^2, \tag{1}$$

where r is the distance from the center of the star and $C = \dot{M}/4\pi m_H V$; expressing $\dot{M}$ and V in units of $10^{-5}\ M_\odot\ \mathrm{yr}^{-1}$ and 10^6 cm s^{-1}, respectively, $C = 3 \times 10^{37}\ \dot{M}_{-5}/V_6$. The kinetic temperature of the gas is assumed to vary as

$$T(r) = T_0\left(\frac{r_0}{r}\right)^m, \tag{2}$$

where T_0, r_0, and m are fitted to various theoretical temperature calculations. For example, in our "standard model" (whose parameters are given in Table 1), we use the results of GS. By specifying the density and temperature distributions, calculations for the photochemical model are reduced to solving a system of ordinary differential equations for the abundances. The inner boundary conditions are specified at a radial distance r_0, well outside the region of dust formation and evolution.

Just beyond the region of dust formation, the wind is assumed to consist only of hydrogen, carbon, oxygen, and nitrogen, with most of the heavier elements in dust. A more comprehensive treatment of the gas phase chemistry of O-rich CSEs, including heavier elements such as S and Si, is postponed to a later paper. The central star is considered to be sufficiently cool that the hydrogen is mainly molecular. Small amounts of atomic hydrogen can have important selective chemical effects (Slavsky and Scalo 1984), but this goes beyond the scope of the present study. In our standard model, we use for simplicity solar abundances for carbon, nitrogen, and oxygen at radius r_0, with all the carbon in CO, all the nitrogen in N_2, and the residual oxygen in H_2O. Condensation of H_2O onto dust grains (Jura and Morris 1985) is assumed to have been completed by the time the molecules reach the region of active chemical activity, i.e., beyond 10^{16} cm. We ignore the production of atoms and molecules such as HCN that might arise in the inner envelope as the result of shocks or other high-excitation processes. In the present calculations, the only gaseous species at r_0 are thus H_2, CO, H_2O, and N_2, with abundances given in Table 1.

The homogeneous, spherically symmetric wind model adopted in this paper (and also in Papers I and II) is greatly oversimplified. Many envelopes are bipolar, and even spherical ones may manifest asymmetries and inhomogeneities close to the star. Asymmetries in the extended chromosphere and dust shell of Alpha Orionis are particularly well documented (Hebden, Eckart, and Hege 1987; Hebden *et al.* 1986; Cheng *et al.* 1986; Bloemhof, Townes, and Vanderwyck 1984; Bloemhof, Danchi, and Townes 1985). A relatively small degree of asymmetry has also been found in images of its outer envelope made in scattered KI radiation (Honeycutt *et al.* 1980; Mauron *et al.* 1984). Strong evidence for clumping close to red giant stars is also provided by observations of SiO masers (Elitzur 1980; Herman and Habing 1985; Alcock and Ross 1986*b*).

The bulk of the present evidence for clumps in spherical CSEs refers to regions close to the star, but the outer envelope may also be clumped. Alcock and Ross (1986*a*) have recently proposed a model for OH masers in which the mass loss occurs in blobs which evolve into transverse platelets under the action of the radial driving force. Although it would be of considerable interest to investigate the chemistry of clumpy CSEs, the development of the required clump dynamics and radiative transfer is beyond the scope of this paper. However, we will comment in § IIIa on some possible effects of clumping on the chemistry.

b) *Ion-Molecule Chemistry*

The chemistry of the outer CSE is illustrated schematically in Figure 1; the associated reaction rates are listed in Table 2 (ion-molecule reactions and recombination) and Table 3 (photoprocesses).

The main building blocks of the chemistry are the three photochains which break down H_2O, CO, and N_2. Photoionization occurs in the first two chains and produces C^+, OH^+, and H_2O^+. The last two ions are rapidly hydrogenated into H_3O^+ in an environment containing H_2. We compare the time scale of hydrogenation with that of recombination:

$$\frac{\tau_{ch}}{\tau_{rec}} = \frac{\beta x_e}{k x(H_2)} = 10^4\ T^{-1/2}\ \frac{x_e}{x(H_2)}, \tag{3}$$

using $\beta = 10^{-5} T^{-1/2}$ cm^3 s^{-1} and $k = 10^{-9}$ cm^3 s^{-1}. For the conditions appropriate to the standard mass-loss rate $\dot{M} = 10^{-5}\ M_\odot\ \mathrm{yr}^{-1}$ ($T \approx 25$ K and $x_e \approx 10^{-6}$ in the region where the ions reach their peak abundance), the requirement $\tau_{ch} < \tau_{rec}$ is satisfied for $x(H_2) \gtrsim 2 \times 10^{-3}$; a similar calculation for $\dot{M} = 10^{-4}\ M_\odot\ \mathrm{yr}^{-1}$ yields $\tau_{ch} < \tau_{rec}$ for $x(H_2) \gtrsim 0.3$. Thus, hydrogenation is more rapid than recombination in any predominantly molecular CSE and in any low to moderate mass-loss CSE in which molecules are detected.

The C^+ ion interacts strongly with H_2O to produce HCO^+ and with OH to produce CO^+, which is hydrogenated to

TABLE 2

PHOTODESTRUCTION RATES

Species	G_{diss}	G_{ion}	d (10^{16} cm)[a]	Reference
CO	1.4 (−10)[b]	...	3.5	1
C	...	3.2 (−10)	3.3	2, 3
H_2O[c]	1.6 (−10)	2.5 (−11)	3.6	4
	2.65 (−10)	...	2.3	
	1.05 (−10)	...	2.4	
OH	2.8 (−10)	1.25 (−11)	2.7	5
O_2	8.9 (−10)	...	2.3	6
N_2	5.0 (−11)	...	2.4	7

[a] Values for $\dot{M} = 10^{-5}\ M_\odot\ \mathrm{yr}^{-1}$; d is proportional to $\dot{M}$.

[b] After blocking of CO bands by H_2 lines (Mamon *et al.* 1987).

[c] H_2O is subdivided into three separate dissociating bands with cross sections 1.75, 0.75, and 0.5 in units of 10^{-17} cm^2, and an ionizing band with a cross section of 1.75 in the same units.

REFERENCES.—(1) Letzelter *et al.* 1987; (2) Burke and Taylor 1979; (3) Cantu *et al.* 1981; (4) Hudson 1971; (5) van Dishoeck and Dalgarno 1984; (6) Black and Smith 1984; (7) van Dishoeck 1987.

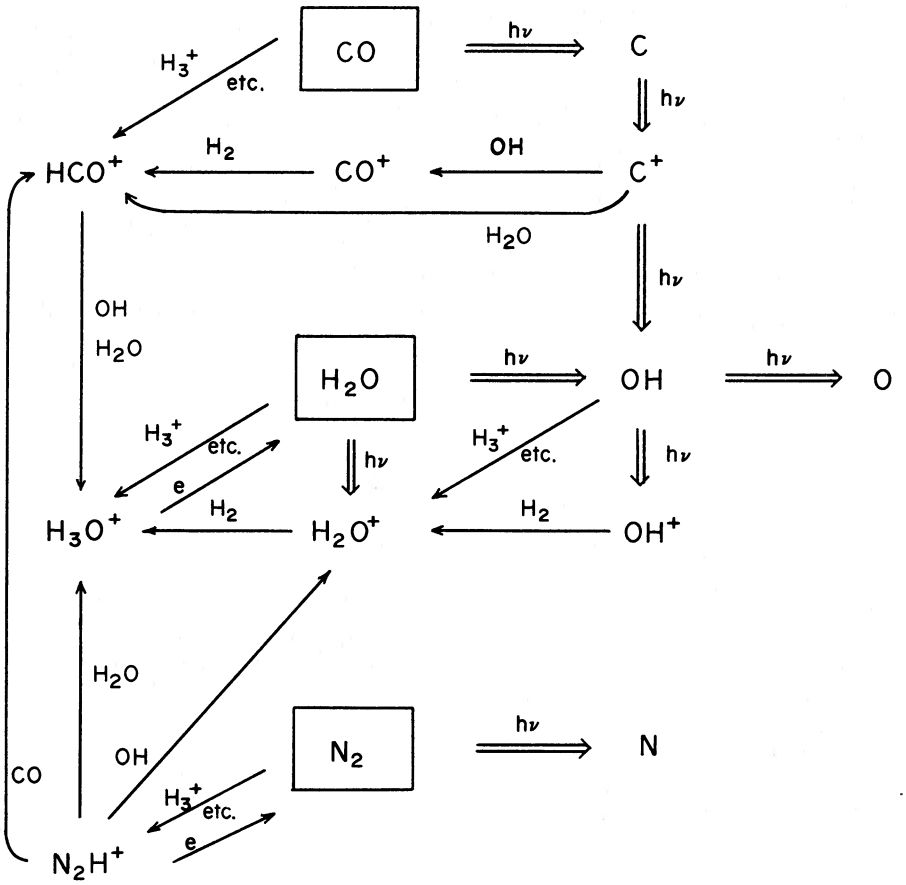

FIG. 1.—Chemical reactions in the model O-rich CSE. The progenitor molecules of the three primary photochains (*double lines*) are shown in *boxes*.

HCO^+; HOC^+ is also produced in the first reaction but is also hydrogenated to HCO^+ (Jarrold *et al.* 1986). The condition for hydrogenation in these cases is similar to that in equation (3). The major mode of destruction of HCO^+ is by proton transfer with H_2O, which yields H_3O^+. The C^+ ion is mainly produced by photodissociation of CO followed by photoionization of C. Thus, the major ions in the model, C^+, HCO^+, and H_3O^+ are all photoproduced.

Cosmic rays generate further ionization by producing H_3^+ from H_2; if the hydrogen were predominantly atomic, the main hydrogen ion would be H^+. The H_3^+ ion undergoes proton transfer with CO, H_2O, and N_2 to yield more HCO^+ and H_3O^+, as well as HN_2^+. These ions undergo further proton transfer, mainly producing more H_3O^+. Cosmic-ray ionization is mainly effective in the inner envelope ($r \lesssim 10^{16}$ cm), where photoprocesses are ineffective due to the shielding of the incoming UV radiation. It is the dominant mechanism for producing H_3^+ and, by interaction with N_2, HN_2^+.

In addition to proton transfer reactions, the main mode of destruction of hydrogenated molecular ions is dissociative recombination; it dominates where $x_e \gtrsim 10^{-6}$ and causes the rapid decrease of these ions at large distances. The only exception is H_3^+, whose recombination rate appears to be characteristic of radiative recombination (Adams and Smith 1987).

Most of the ionic reaction rates listed in Table 3 have been measured in the laboratory. In those cases where experimental values were not available, approximate rates were adopted from simple theoretical considerations, usually from Herbst and Leung (1986). Although the dominant moleculer ions interact with neutral species containing S and Si, their omis-

TABLE 3

REACTION RATES

	Reaction	k (100 K) ($cm^3\ s^{-1}$)	α[a]	Reference
1.	$C^+ + H_2O \rightarrow HCO^+ + H$	4.7 (−9)	−0.5	1
2.	$C^+ + OH \rightarrow CO^+ + H$	9.9 (−9)	−0.5	1
3.	$C^+ + O_2 \rightarrow CO^+ + O$	4.0(−10)	0	2
4.	$C^+ + O_2 \rightarrow O^+ + CO$	6.0(−10)	0	2
5.	$H_3^+ + H_2O \rightarrow H_3O^+ + H_2$	6.9 (−9)	−0.5	1
6.	$H_3^+ + OH \rightarrow H_2O^+ + H_2$	1.6 (−8)	−0.5	1
7.	$H_3^+ + O \rightarrow OH^+ + H_2$	8.0(−10)	0	2
8.	$H_3^+ + CO \rightarrow HCO^+ + H_2$	1.6 (−9)	0	2
9.	$H_3^+ + C \rightarrow CH^+ + H_2$	2.0 (−9)	0	1
10.	$H_3^+ + N_2 \rightarrow HN_2^+ + H_2$	1.8 (−9)	0	2
11.	$HCO^+ + H_2O \rightarrow H_3O^+ + CO$	3.5 (−9)	−0.5	1
12.	$HCO^+ + OH \rightarrow H_2O^+ + CO$	8.1 (−9)	−0.5	1
13.	$HN_2^+ + H_2O \rightarrow H_3O^+ + N_2$	4.5 (−9)	−0.5	2
14.	$HN_2^+ + OH \rightarrow H_2O^+ + N_2$	8.1 (−9)	−0.5	1
15.	$HN_2^+ + O \rightarrow OH^+ + N_2$	1.4(−10)	0	2
16.	$HN_2^+ + CO \rightarrow HCO^+ + N_2$	8.8(−10)	0	2
17.	$O + OH \rightarrow O_2 + H$	3.3(−11)	−0.5[b]	3
18.	$H_3^+ + e^- \rightarrow H_2 + H$	1.7(−11)	−0.5	4
19.	$H_3O^+ + e^- \rightarrow H_2O + H$	8.3 (−7)	−0.5	5, 6
	$\rightarrow OH + H_2$	1.7 (−7)	−0.5	
20.	$C^+ + e^- \rightarrow C$	9.7(−12)	−0.625	7
21.	$HCO^+ + e^- \rightarrow CO + H$	3.3 (−7)	−1	8
22.	$HN_2^+ + e^- \rightarrow N_2 + H$	2.4 (−7)	−1	8
	$\rightarrow N + N + H$	2.4 (−7)	−1	

[a] $k(T) = k(100\ \mathrm{K})T^{\alpha}$.

[b] This reaction has an activation energy of ~80 K.

REFERENCES.—(1) Herbst and Leung 1986; (2) Anicich and Huntress 1986; (3) Black and Smith 1984; (4) Adams and Smith 1987; (5) Mul *et al.* 1983; (6) Bates 1986; (7) Aldrovandi and Pequignot 1973; (8) Smith and Adams 1984.

sion from the model generates only small errors in the molecular ion abundances because of the low abundances of gaseous S and Si. All ion molecule reactions with H_2O and OH have been scaled up by a factor $(300/T)^{1/2}$ relative to their rates measured at 300 K, in accord with theoretical (e.g., Clary 1985) and experimental (Adams, Smith, and Clary 1985; Adams and Smith 1987) studies of reactions of ions with neutral molecules possessing large dipole moments. The branching ratio for dissociative recombination of H_3O^+ is based on the recent work of Bates (1986). Unlike the situation for shielded dense interstellar clouds (Sternberg, Dalgarno, and Lepp 1987), our results do not depend sensitively on this parameter.

Finally, neutral-neutral reactions generally play a negligible role here, because their activation energies are usually too large for the temperatures found in the outer parts of CSEs. The one exception is the reaction $O + OH \rightarrow O_2 + H$, which produces significant ($\sim 10^{-5}$) amounts of O_2; the abundance of O_2 is limited by its destruction by C^+ and by photodissociation in the outer envelope.

b) *Photorates and Shielding*

The most important rates are given in Table 2 with references for the underlying cross sections. The unshielded rates have been calculated with the Jura (1974) interstellar radiation field below 1100 Å and with the "Jura-Habing" interpolation (Glassgold and Langer 1974; curve 3 of Fig. 1) at longer wavelengths. This representation of the interstellar radiation is essentially the same as in Draine (1978) and was also used in Papers I and II. The rate for N_2 is very uncertain (van Dishoeck 1987), and we have adopted her minimum value.

The UV radiation that contributes to the photodissociation and photoionization rates given in Table 2 is shielded by dust and by abundant gas phase species. The dust shielding is approximated by an exponential attenuation factor $e^{-d/r}$, as in Papers I and II. The depth d is the distance at which the incoming radiation reaches an optical depth of order unity for the process and species in question. The values of d given in Table 1 are based on the properties of interstellar dust, but circumstellar dust could be significantly different and d should be varied in attempts to fit the observations.

For continuum photoprocesses, self-shielding is included with the following iterative procedure. Each self-shielding species j is subdivided into wavelength intervals k in which the photodissociation cross section is roughly constant, and the optical depth $\tau_{j,k}$ of species j and wavelength interval k is treated as an additional dependent variable. In the zeroth order, we integrate the system of abundances and optical depths from r_0 to r_{max} assuming no self-shielding, i.e., $\tau_{j,k}^{(0)} = 0$ throughout the envelope. We then iterate using

$$\tau_{j,k}^{(i+1)}(r_0) = \sigma_{j,k} \int_{r_0}^{r_{max}} x_j^{(i)} n(r) dr ,$$

where $\sigma_{j,k}$ is the cross section of the jth species in the kth wavelength interval. The iterations are terminated once the condition

$$|\tau_{j,k}^{(i+1)}(r_0) - \tau_{j,k}^{(i)}(r_0)| < 10^{-3}$$

is satisfied, which usually takes less than 12 steps. Self-shielding is important only for species with large column densities and cross sections, and it is applied here only to H_2O, using three dissociation bands with the cross sections listed in Table 2.

Self-shielding of CO is now understood to occur mainly through absorption by lines, rather than by continuum absorption, as discussed by Glassgold, Huggins, and Langer (1985). Because CO photodissociation provides the main source of C^+ in O-rich envelopes, which itself is the main source for the formation of HCO^+, an accurate treatment of CO line self-shielding is fundamental to this study. Morris and Jura (1983) developed the theory of line self-shielding of CO for CSEs, using the Sobolev approximation, and Mamon, Glassgold, and Huggins (1987) have adapted their formulation to the recent far-UV absorption and fluorescence measurements of Letzelter *et al.* (1987). According to these experiments, there are 34 CO bands which contribute significantly to the dissociation of CO by interstellar UV radiation, with a mean oscillator strength 1.1×10^{-2}. However, a significant number of these bands will be blocked by nearly coincident Lyman and Werner bands of H_2 and Lyman lines of H. The number of blocked bands depends on position but, for the region of primary interest (where H_3O^+ and HCO^+ are abundant), about 16 bands are involved. Thus, our standard model is based upon 23 bands with mean oscillator strength 1.4×10^{-2}, corresponding to an unshielded photodissociation rate of 1.4×10^{-10} s^{-1} (see Mamon, Glassgold, and Huggins 1987, for details).

III. RESULTS AND DISCUSSION

a) *Abundances*

The computed abundances for the standard model (parameters and rates in Tables 1–3) are shown in Figure 2; the N_2 photochain and several minor species have been omitted for clarity. The spatial distribution of CO shown in Figure 2*a* is much more extended than that of H_2O; this reflects the difference between line self-shielding of CO and continuum self-shielding of H_2O. Another consequence of CO line self-shielding is the unusual shape of the C distribution, already noted for C-rich CSEs (Paper II).

A result of immediate interest in the distribution of electrons and ions is the high abundance (up to $\sim 10^{-7}$) of both H_3O^+ and HCO^+ at intermediate distances, as seen in Figure 2*b*. The C^+ ion is also relatively abundant in this region and, consequently, the electron fraction reaches $\sim 5 \times 10^{-6}$ at the HCO^+ peak. In the region where it is rising, the HCO^+ distribution has the unusual property that $x(HCO^+) \approx x(C^+)$. This occurs because HCO^+ is both formed from and destroyed by H_2O (reactions 1, 2, 11, and 12 in Table 3), so that

$$\frac{x(HCO^+)}{x(C^+)} \approx \frac{k_1 + yk_2}{k_{11} + yk_{12}} \approx 1 ,$$

where $y = x(OH)/x(H_2O)$. The abrupt fall of HCO^+ is due to similar decreases in its progenitors, H_2O and OH, accompanied by a rapid increase in x_e, which makes dissociative recombination the main mechanism for its destruction. Further out in the envelope, where $x(H_3^+)$ becomes appreciable, HCO^+ is replenished somewhat by reaction 6, $H_3^+ + CO \rightarrow HCO^+ + H_2$, which is the dominant formation mechanism in C-rich envelopes, but its abundance remains $< 10^{-10}$. Although molecular ions are mainly produced by cosmic rays in the inner envelope, e.g., H_3O^+ (see Fig. 2*b*), their peak abundances, which are reached at intermediate distances, are a consequence of photoionization of H_2O and C (the latter from photodissociation of CO).

It is interesting to compare these results with those obtained recently for C-rich envelopes. The analog of H_3O^+ in C-rich CSEs is $C_2H_2^+$, and its abundance also reaches the 10^{-7} level

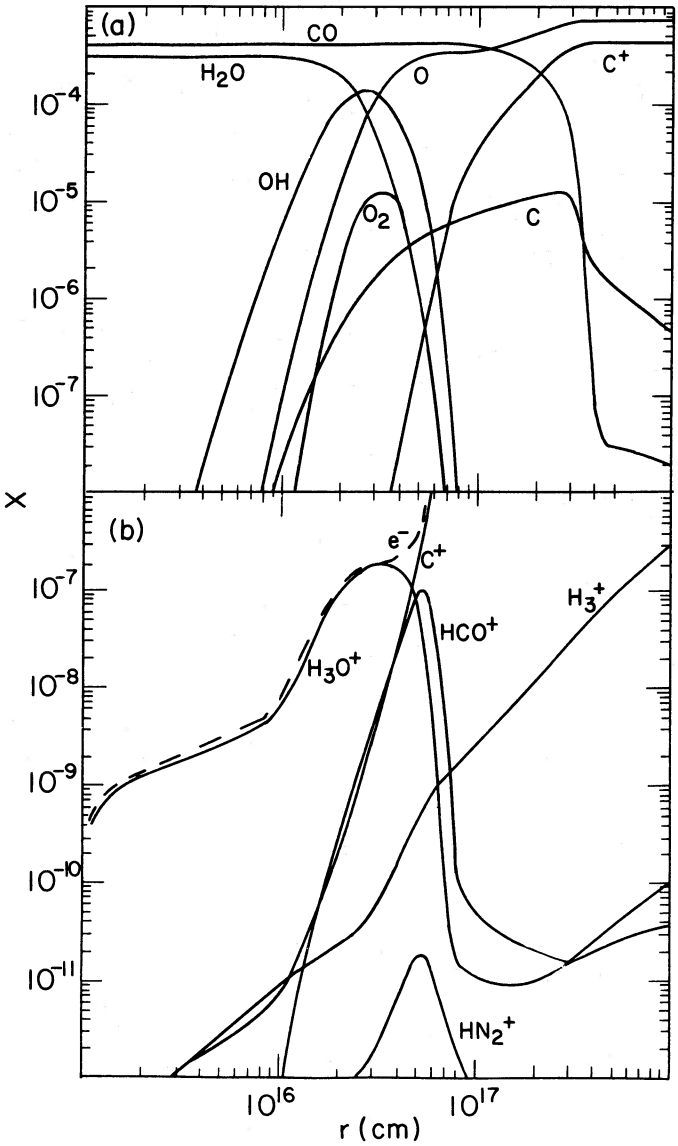

FIG. 2.—Chemical abundances for the standard O-rich CSE (Table 1): (*a*) CO, H_2O, and O_2 photochains; (*b*) ions and electrons.

(see Papers I and II). The smaller photoionization cross section of H_2O is compensated by its larger initial abundance, relative to C_2H_2. In a C-rich envelope, the process analogous to $C^+ + H_2O \rightarrow HCO^+ + H$ is $C^+ + C_2H_2 \rightarrow C_3H^+ + H$. Subsequent hydrogenation by H_2 leads to $C_3H_2{}^+$ and then to C_3H by recombination (Nejad, Millar, and Freeman 1984). In C-rich CSEs, $x(C_3H_2{}^+)$ reaches $\sim 10^{-8}$; the larger abundance of HCO^+, its analog in O-rich envelopes, is due to the polar nature of H_2O and OH, which leads to larger rates for its formation.

As the mass-loss rate is increased, the shielding of both H_2O and CO increases, and the photochains are displaced to larger radii. This is illustrated in Figure 3 for both H_3O^+ and HCO^+. The peak abundances are all of the order of 10^{-7} for the range in $\dot{M}$ used in Figure 3, 10^{-7} to 10^{-4} $M_\odot$ yr^{-1}, and they decrease with increasing $\dot{M}$. The distribution of HCO^+ is more sharply peaked than that of H_3O^+, and its maximum abundance is more affected by the mass-loss rate. These differences arise because the HCO^+ distribution is determined by C^+ and line shielding of CO, whereas the H_3O^+ distribution is determined by H_2O and dust shielding. The electrons that destroy H_3O^+ have an abundance $x_e \approx x(H_3O^+)$, which leads to $x(H_3O^+) \propto n^{-1/2} \approx \dot{M}^{-1/2}$. The dependence on $\dot{M}$ is weaker than this, however, because dust shielding moves the distribution farther out to lower densities. The peak abundance of HCO^+ is essentially the same as that of C^+ at the position where recombination begins to dominate destruction by reactions with H_2O and OH. For line self-shielding of CO, the abundance of C^+ in this region decreases roughly as $\dot{M}^{-1}$, in accord with Figure 3.

Because the HCO^+ abundance in O-rich CSEs depends directly on C^+, it is important to determine how $x(HCO^+)$

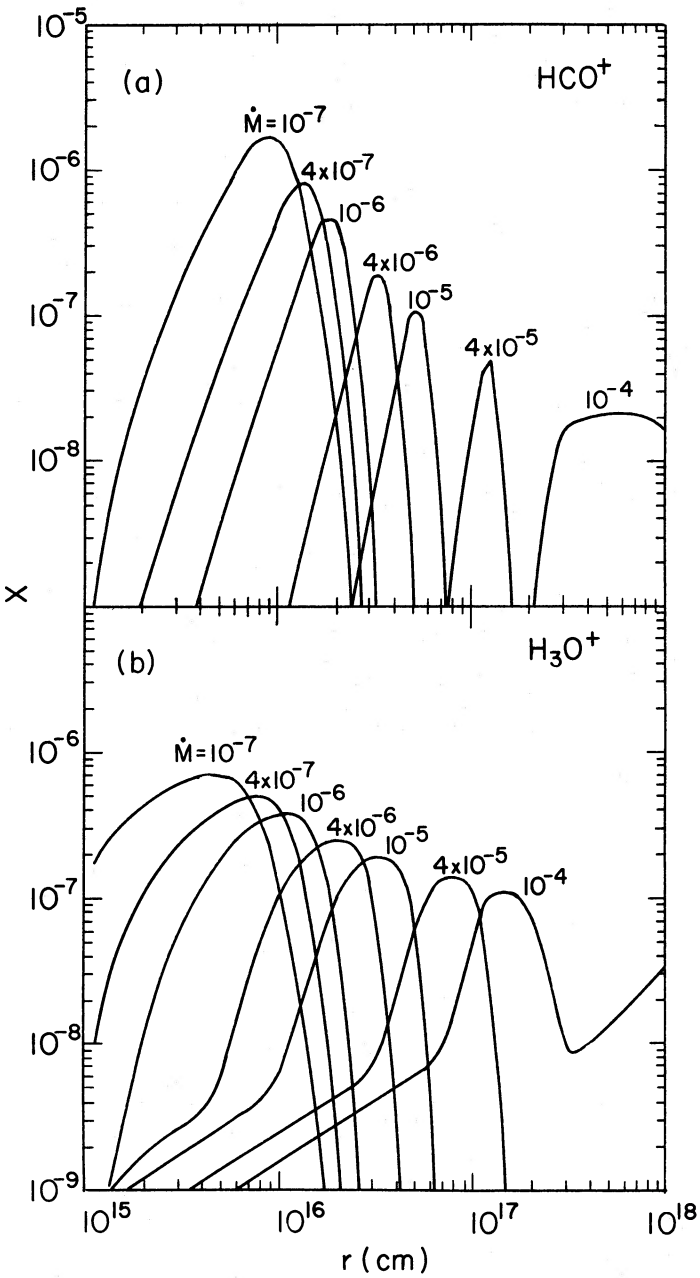

FIG. 3.—Ion abundance distributions for three different mass-loss rates (in units of $M_\odot$ yr^{-1}): (*a*) HCO^+, (*b*) H_3O^+

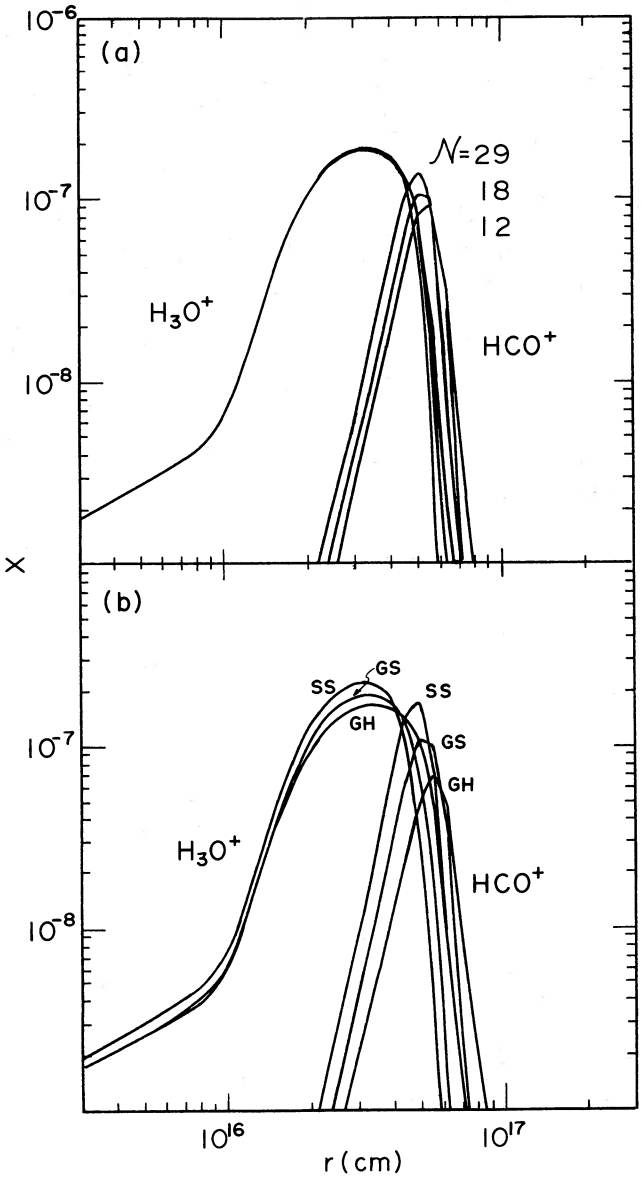

FIG. 4.—Abundance distributions of HCO^+ and H_3O^+ for (*a*) variations in the number $\mathcal{N}$ of bands effective in the photodissociation of CO ($\mathcal{N} = 23$ is the standard model), and (*b*) three different temperature distributions—GS: $T = 550\, r_{15}^{-0.7}$ K (Goldreich and Scoville 1976); SS: $T = 805\, r_{15}^{-0.6}$ K (Slavsky and Scalo 1984); GH: $T = 800\, r_{15}^{-1.0}$ K (Glassgold and Huggins 1986*b*).

depends on the parameters used in the theory of line-shielding of CO. Figure 4*a* shows the HCO^+ abundance for three values of the number of bands $\mathcal{N}$ and the corresponding unshielded rate of CO photodissociation G(CO): the standard values given in § II*d* ($\mathcal{N} = 23$, $G = 1.4 \times 10^{-10}$ s^{-1}), the unblocked values ($\mathcal{N} = 34$, $G(\mathrm{CO}) = 2.0 \times 10^{-10}$ s^{-1}), and the case where more distant bands as well as nearly coincident ones are blocked ($\mathcal{N} = 17$, $G(\mathrm{CO}) = 1.1 \times 10^{-10}$ s^{-1}). The differences are small and the main effect of decreasing $\mathcal{N}$ is to move the $CO \rightarrow C^+$ transition to slightly larger distances where the larger C^+ abundance leads to smaller HCO^+ abundances.

The temperature distribution in the envelope affects the computed abundances mainly through the temperature dependence of the chemical reaction rates. We illustrate in Figure 4*b* the effects of choosing different temperature distributions on the abundances of H_3O^+ and HCO^+. For comparison with the standard temperature distribution of GS, we use those derived by Slavsky and Scalo (1984) for general O-rich CSEs and by Glassgold and Huggins (1986*b*) for α Ori. The changes in the peak abundances of H_3O^+ and HCO^+ correlate with decreasing temperature, and arise mainly from the T^{-1} and $T^{-1/2}$ dependences of the recombination rates of HCO^+ and H_3O^+, respectively.

Although the above results are based on a highly idealized model, qualitative aspects of the generalized photochemical model probably apply to other models such as the clumpy wind mentioned in § II. In particular, ion-molecule reactions should still produce substantial levels of H_2O^+ and HCO^+ in O-rich CSEs, determined in large part by C^+ ions produced by photodissociation of CO. We can attempt to illustrate some of the effects of clumping with an extreme version of the Alcock and Ross (1986*a*) model in which there are a large number of high-density platelets. The most important change in our model probably occurs in the self-shielding of the CO dissociating radiation. The transfer of the continuum radiation responsible for the dissociation and ionization of H_2O will be altered relatively little. Because the UV line radiation traveling in tangential directions is most effective in dissociation, the CO in thin, dense platelets will be more effective in shielding than a uniform wind.

Increased shielding of the CO dissociating radiation would imply that the chemically important C^+ ion occurs further out in this type of clumpy envelope as compared to a uniform one. As a consequence, production of HCO^+ would occur at larger distances as would destruction of both HCO^+ and H_3O^+. We would then expect the peak abundance of HCO^+ distribution to be about the same but its brightness temperature to be decreased because of weaker excitation. The H_3O^+ would extend to larger distances and reach a larger peak abundance, and the chances for detecting this ion in O-rich CSEs might be increased somewhat (see the discussion of observability of molecular ions in § III*b* below). These remarks about the ion-molecule chemistry of clumpy envelopes are very preliminary. They are likely to be sensitive to the physical properties of the clumps. A deeper understanding of the effects of clumping on circumstellar must await detailed calculations.

b) Observability

Consistent with our focus on ionization, we discuss the prospects for observing molecular ions in O-rich CSEs. There are only two real possibilities, H_3O^+ and HCO^+ because, as will be shown below, the other abundant molecular ion, H_3^+, has a peculiar spatial distribution which mediates against its detection.

i) H_3^+

The theory of the abundance of H_3^+ is basically the same for O-rich and C-rich envelopes: production by cosmic rays and destruction by proton transfer reactions with neutrals. Its density is given by the simple expression

$$n(H_3^+) = \frac{\zeta}{\sum_i k_i x_i},$$

where ζ is the cosmic ray ionization rate of H_2 (per hydrogen nucleus), and k_i and x_i are, respectively, the rate constants and abundances of the neutral species that destroy H_3^+. The denominator does not vary much throughout the envelope

because both progenitor molecules and photofragments react strongly with H_3^+, with rate constants typically $\sim 10^{-9}$ cm^3 s^{-1}. Consequently the abundance of H_3^+ varies roughly as r^2, as is shown in Figure 2 (see also eq. [8] of Paper I). The jump in $x(H_3^+)$ in the region 3–7 $\times 10^{16}$ cm occurs because, according to Table 3, the destruction by O is less effective than by H_2O and OH. The column density is given by

$$N(H_3^+) = \frac{\zeta r_m}{k\bar{x}} = 10^{13} \left(\frac{\zeta_{-17} r_{m18}}{k_{-9} x_{-3}} \right) \text{cm}^{-2} ,$$

where r_m is the outer boundary of the envelope and all parameters are measured in cgs units with powers of 10 indicated by subscripts. The column density is independent of mass-loss rate and, as discussed in Paper I for C-rich envelopes, its order of magnitude is too small for the infrared detection of H_3^+ with present instrumentation.

ii) HCO^+

The lowest $J = 1 \rightarrow 0$ rotational transition of HCO^+ at 89.2 GHz provides the best method for detecting this ion in CSEs, and several detections have been made recently with the IRAM 30 ms telescope (Morris *et al.* 1987; Bachiller, Bujarrabal, and Gomez-Gonzalez 1987; Guilloteau, Omont, and Lucas 1987). Most of the CSEs in which HCO^+ has been detected so far appear to be high-excitation objects such as bipolar and/or young planetary nebulae. In this paper we restrict the discussion to spherically symmetric envelopes without internal sources of ionization. We follow the methods of § III of Paper I for calculating the brightness temperature of this line. There are two important differences in applying the methods of Paper I to O-rich envelopes. First, the large abundance of HCO^+ implies that the line is generally optically thick at the peak of the HCO^+ abundance distribution. The excitation temperature is then a sensitive function of various parameters (e.g., Morris and Alcock 1977), particularly the infrared excitation rate, and population inversion often occurs at some locations. Thus the computed brightness temperatures are less certain than for C-rich envelopes. Second, there is no equivalent of the very luminous C-rich CSE, IRC +10216, among the nearby O-rich envelopes. This situation is partly compensated by the predicted increase of the HCO^+ abundance for small mass-loss rates. The best opportunities for detecting HCO^+ in O-rich CSEs appear to be nearby Mira stars with $\dot{M} \approx 10^{-7}$ to 10^{-6} $M_\odot$ yr^{-1} and $d \approx 100$–200 pc, rather than the massive but relatively distant OH/IR envelopes e.g., IRC +10011 ($\dot{M} \approx 10^{-5}$ $M_\odot$ yr^{-1}, $d = 500$ pc) and NML Tau ($\dot{M} \approx 10^{-6}$ $M_\odot$ yr^{-1}, $d \approx 300$ pc). The case of *o* Cet ($\dot{M} \approx 6 \times 10^{-7}$ $M_\odot$ yr^{-1}, $d = 80$ pc) is interesting, although its bright UV companion may alter the photochemistry.

For IRC +10216, the IR pumping of HCO^+ is dominated by the ν_2 bending mode near 11 μm, with an appreciable contribution of the ν_3 mode near 5 μm (Paper I). The same is probably true for OH/IR stars, but in Miras the ν_1 ($\lambda \approx 3.2$ μm) and the ν_3 modes dominate. For prominent nearby O-rich envelopes (e.g., *o* Cet, R Cas, NML Tau, IRC +10011) we estimate that the IR pumping rate of HCO^+ is a factor 5–10 smaller than the one used in Paper I.

Figure 5 displays the on-source, beam averaged brightness temperature T_{MB} at the center of the $J = 1 \rightarrow 0$ HCO^+ line for a 30 m telescope, as a function of the distance to the star. Values for other telescope diameters D can be easily deduced by scaling because the results depend only on d/D. The calculations have been performed for the IR pumping rate R_0 of Paper I (*dashed curves*), and for the more realistic case $R_0/10$ (*solid curves*).

The results depend only mildly on the mass loss rate for $\dot{M} < 10^{-5}$. The peak density $n(HCO^+)$ decreases slowly with $\dot{M}$ but is compensated to a large degree by the increasing extent of the HCO^+ distribution. However, for $\dot{M}$ approaching 10^{-4} $M_\odot$ yr^{-1}, the large HCO^+ shell can be partially resolved and T_{MB} decreases with decreasing distance d as the observations increasingly sample the hole in the HCO^+ distribution. Compared to C-rich envelopes with the same mass-loss rate (Papers I and II), the emission is much stronger for O-rich CSEs (e.g., by a factor ~ 20 for $\dot{M} = 10^{-5}$ $M_\odot$ yr^{-1}). However, the increase is not proportional to the peak abundance ratios (~ 400), mainly because the line is optically thick. Figure 5 also illustrates the strong dependence on the IR excitation rate, and hence the sensitivity of the results to the precise value of the IR dipole moment and possibly the phase of the star.

The 30 m telescope (FHWM beam size of 25″ at 89 GHz) is unable to resolve the HCO^+ emission expected for most of the familiar O-rich envelopes, including NML Tau and IRC +10011. It could marginally resolve the emission from *o* Cet, where the calculated radius of the HCO^+ distribution is $\sim 15''$, and the beam averaged emission has a FWHM width of 25″. The brightness temperature distribution for a massive envelope ($\dot{M} = 10^{-4}$ $M_\odot$ yr^{-1}) is very extended (the HCO^+ density peaks at 3×10^{17} cm) and, at a typical distance of 1 kpc, the emission is extremely weak (~ 2 mK) and probably presently undetectable.

In summary, the large abundance of HCO^+ in O-rich CSEs does not imply that the brightness temperature of the $J = 1 \rightarrow 0$ line is large. For a typical case of an object with $\dot{M} = 10^{-5}$ $M_\odot$ yr^{-1}, $d = 500$ pc, and $R = R_0/5$, the calculated mean brightness temperature for the 30 m telescope is only about 0.01 K. Thus the present theory is not in contradiction with the recent reports of nondetections of HCO^+ in IRC +10011 and NML Tau with an rms noise temperature of ~ 0.015 mK (Guilloteau, Omont, and Lucas 1987). The line may be stronger in less massive nearby Mira envelopes. The production of HCO^+ in bipolar envelopes probably involves the specific, high-excitation (e.g., shocks) conditions characteristic of these systems, and is beyond the scope of the present investigation.

iii) H_3O^+

The oxonium ion H_3O^+ plays an important role in the synthesis of interstellar molecules based on ion-molecule reactions (Herbst and Klemperer 1973; Watson 1973; Dalgarno, Oppenheimer, and Berry 1973). Hollis *et al.* (1986) and Wootten *et al.* (1986) have detected a line near 1 mm in the Kleinman-Low nebula in Orion which may be from H_3O^+, but a definitive detection requires more than one line. The peak abundances of H_3O^+ (10^{-7}) in our theory of O-rich CSEs are several orders of magnitude larger than obtained in models of interstellar clouds (e.g., Leung, Herbst, and Huebner 1984; Millar and Nejad 1985). The essential difference is that, in CSEs, H_3O^+ is predominantly produced by photoionization of H_2O and OH (see Fig. 1), rather than by cosmic rays.

The oxonium ion is isoelectric with ammonia and has a similar pyramidal structure with four vibrational modes (ν_1, ν_2, ν_3, and ν_4) and with a characteristic inversion spectrum. Only the ν_2 bending-inversion mode is not blocked by Earth's atmosphere, and its splitting in the ground state is 55.34 cm^{-1} (Liu and Oka 1985). Liu, Oka, and Sears (1985) have analyzed the

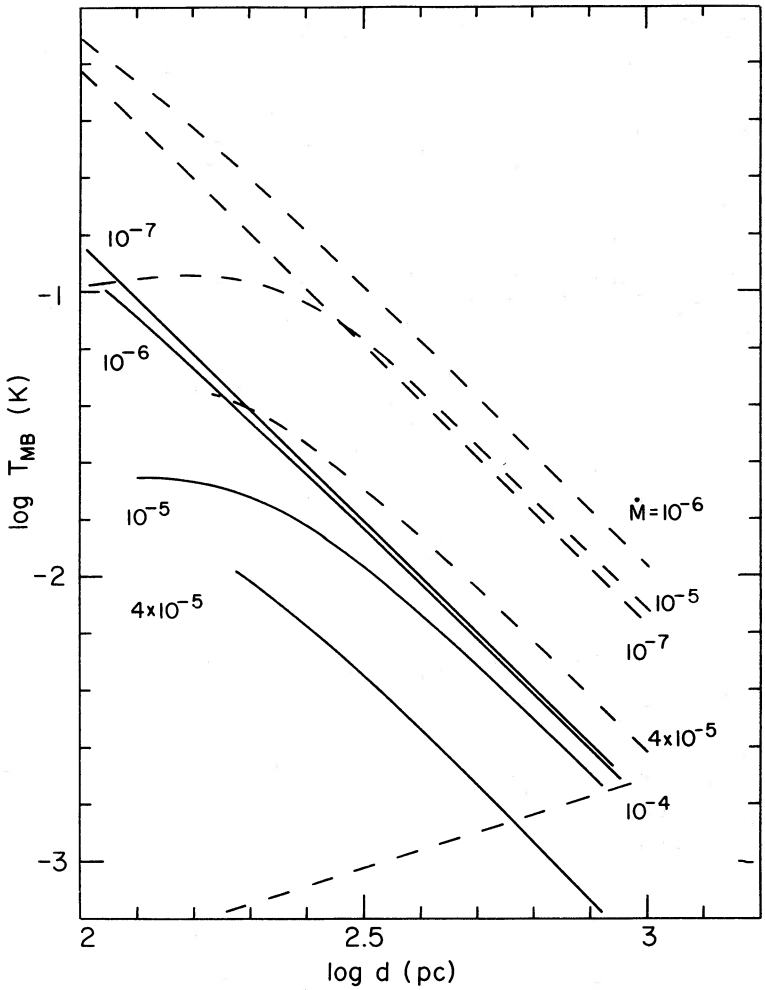

FIG. 5.—Values of the on-source beam-averaged brightness temperature for different mass-loss rates ($M_\odot$ yr^{-1}) and different stellar infrared fluxes ($R = R_0$: *dashed curves* and $R = R_0/10$; *solid curves*) as a function of the distance d to the source for a 30 m telescope. The results depends only on d/D and can thus easily be extended to other values of the telescope diameter D.

recent measurements of the v_2 bands and obtained accurate spectroscopic constants and frequencies for the four lowest ones. The transitions of primary astrophysical interest occur at sub-millimeter and mid-infrared (1^-–0^+ at 10 μm and 1^+–0^- at 17 μm) wavelengths and are shown in Figure 6*a*. Many transitions are observable from the ground.

Figure 6*b* gives the levels which lie less than 200 cm^{-1} above the $J = 1$, $K = 1^+$ ground state; these are the most likely initial states for emission and absorption lines that might be detectable in a CSE. The four transitions marked with double arrows have been measured in the laboratory (Plummer, Herbst, and de Lucia 1985; Bogey *et al.* 1985), and have wavelengths between 0.75 and 1 mm. The transition at 307 GHz ($11^- \rightarrow 21^+$) has been searched for in interstellar clouds (Hollis *et al.* 1986; Wootten *et al.* 1986); the upper level in this case is about 80 K above the ground state. The next lowest transition ($00^- \rightarrow 10^+$), whose upper level is at 56 K, has a frequency of 985 GHz (305 μm), and its detection would have to be attempted from space, e.g., with the Kuiper Airborne Observatory.

The transition dipole moments calculated for the v_2 band are large (Botschwina, Rosmus, and Reinsch 1983); for the transitions of interest $\mu(0^-$–$0^+) = 1.438D$, $\mu(1^-$–$0^+) = 0.302D$, and $\mu(1^+$–$0^-) = 0.673D$. These values imply that the millimeter and submillimeter transitions of H_3O^+ in CSEs are excited by the absorption of infrared radiation rather than by collisions. Because O-rich CSEs emit strongly at 10 μm and 17 μm (Forrest, McCarthy, and Houck 1979), both the 1^+–0^- and 1^-–0^+ v_2 bands are likely to be effective in absorbing infrared radiation. A detailed calculation of the excitation of the rotational bands of H_3O^+ is beyond the scope of this paper, but the underlying physical processes appear to be favorable for relatively strong excitation. Emission in the lowest submillimeter transitions of H_3O^+ is probably stronger than from HCO^+, because the transition dipole moments are larger and because H_3O^+ is located closer to the star.

In principle, H_3O^+ could also be detected by infrared absorption techniques as have other circumstellar molecules, particularly toward IRC +10216 (see Betz 1987 for a recent review). We have estimated the absorption coefficients for transitions from low-lying levels (80 K above the ground state) using the measured frequencies for the 1^-–0^+ and 1^+–0^- bands (Liu, Oka, and Sears 1985), the calculated dipole moments of Botschwina, Rosmus, and Reinsch (1983), the Hönl-London factors in Herzberg (1945), and a turbulent (Doppler) broadened line with FWHM width of 1 km s^{-1}. The typical order of magnitude of the absorption cross section is

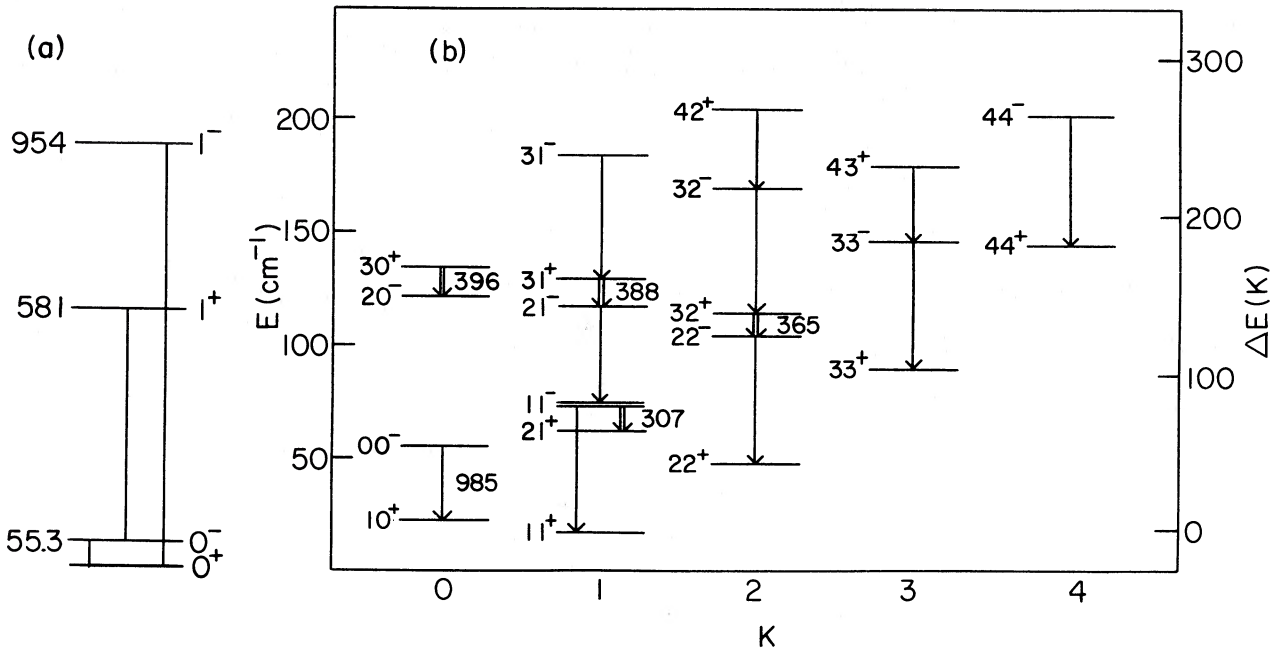

FIG. 6.—Energy levels of the ν_2 mode of H_3O^+: (*a*) four lowest vibrational levels with transitions of astrophysical interest, 0^-–0^+ (mm and sub-mm), 1^+–0^- (10 μm), 1^-–0^+ (20 μm); (*b*) low-lying levels and transitions for the 0^-–0^+ band. Fig. 6*a* is patterned after Liu *et al.* (1985) and Fig. 6*b* after Bogey *et al.* (1985). The energy units are cm^{-1} throughout.

10^{-15} cm^2 and, if the corresponding populations are not too small, a column density of 10^{14} cm^{-2} might be sufficient to give a detectable absorption with a sensitive, high-resolution ($\lambda/\Delta\lambda \approx 3 \times 10^5$) spectrometer. The column densities of H_3O^+ calculated in our model do reach this level, with the major contributions coming from the peak in the H_3O^+ abundance. The excitation of H_3O^+ will change with mass-loss rate because the position of the abundance peak increases with $\dot{M}$, as shown in Figure 3*b*. For small $\dot{M}$, many levels are excited in the interior of the envelope and the absorption coefficients are then very small. For large $\dot{M}$ (10^{-5} to 10^{-4} $M_\odot$ yr^{-1}), the H_3O^+ peak is sufficiently distant that the populations of the two lowest levels may be large enough to produce a detectable amount of absorption. Nonetheless, infrared detection of H_3O^+ column densities of even a few times 10^{14} cm^{-2} will still be difficult. In this context, it is worth noting that the current sensitivity for the detection of circumstellar molecules by infrared absorption in IRC +10216 is $\sim 10^{15}$ cm^{-2} (Betz 1987).

IV. SUMMARY

We have developed a model for the ionization of O-rich CSEs based upon the photochemical model, using the methodology developed for C-rich CSEs (Papers I and II). We again find a rich ion-molecule chemistry that is strongly dependent on position within the envelope. This chemistry is driven mainly by photoprocesses, supplemented by cosmic-ray ionization. The overall spatial distribution of the ionization is similar to that in C-rich CSEs, although it is generated by different chemical species.

An important aspect of O-rich envelopes is that large peak abundances ($\sim 10^{-7}$) are predicted for the polar molecular ions, H_3O^+ and HCO^+. The H_3O^+ ion is produced by photoionization of H_2O and OH, whereas HCO^+ is formed by reactions of H_2O and OH with C^+ (produced in the CO photodissociation chain). The present calculations suggest that the abundance of H_3O^+ is an order of magnitude too low to be detectable at the present time in IR absorption, and probably in millimeter emission as well. However, our understanding of the excitation conditions of H_3O^+ in O-rich CSEs is incomplete at best, and we believe that an effort should still be made to detect its emission in submillimeter lines.

We do find that HCO^+ is abundant enough to be detectable in the $J = 1 \rightarrow 0$ transition at 89.2 GHz as long as the envelope is not too massive ($\dot{M} \lesssim 10^{-5}$ $M_\odot$ yr^{-1}) or distant ($d < 1$ kpc), but its relatively large abundance does not yield particularly strong lines because of optical thickness and excitation effects. It is thus unfortunate that there is no counterpart among O-rich envelopes to the nearby and extremely luminous C-rich envelope, IRC +10216. Nevertheless, our colleagues at the IRAM 30 m telescope have succeeded in detecting this line in a handful of cases. Further observations of molecular ions, as well as theoretical calculations extending the ones presented here, should elucidate their role in determining the physical and chemical properties of red giant winds.

We would like to thank M. Jura for helpful comments and R. Lucas for his help in the use of his molecular excitation and line formation codes. This work was supported in part by NASA grant NAGW 630.

REFERENCES

Adams, N. G., and Smith, D. 1987, in *Astrochemistry*, ed. M. S. Vardya and S. P, Tarafder (Dordrecht: Reidel), p. 1.
Adams, N. G., Smith, D., and Clary, D. C. 1985, *Ap. J. (Letters)*, **296**, L31.
Alcock, C., and Ross, R. 1986*a*, *Ap. J.*, **305**, 837.
Alcock, C. 1986*b*, *Ap. J.*, **310**, 838.
Aldrovandi, S. M. V., and Pequignot, D. 1973, *Astr. Ap.*, **25**, 137.
Anicich, V. G., and Huntress, W. T. 1986, *Ap. J. Suppl.*, **62**, 553.
Bachiller, R., Bujarrabal, V., and Gomez-Gonzalez, J. 1987, in preparation.

Bates, D. R. 1986, *Ap. J.* (*Letters*), **306**, L45.
Betz, A. 1987, in *Astrochemistry*, ed. M. S. Vardya and S. P. Tarafder (Dordrecht: Reidel), p. 327.
Black, J. H., and Smith, P. L. 1984, *Ap. J.*, **277**, 562.
Bloemhof, E. E., Danchi, E. E., and Townes, C. H. 1985, *Ap. J.* (*Letters*), **299**, L37.
Bloemhof, E. E., Townes, C. H., and Vanderwyck, A. H. B. 1984, *Ap. J.* (*Letters*), **276**, L21.
Bogey, M., Demuynck, C., Denis, M., and Destombes, J. L. 1985, *Astr. Ap.*, **148**, L11.
Botschwina, P., Rosmus, P., and Reinsch, E. A. 1983, *Chem. Phys. Letters*, **103**, 299.
Bowers, P. F., Johnston, K. J., and Spencer, J. H. 1981, *Nature*, **291**, 382.
Burke, P. G., and Taylor, K. T. 1979, *J. Phys.*, **B18**, 2971.
Cantu, A. M., Mazzoni, M., Pettini, M., and Tozzi, G. P. 1981, *Phys. Rev. A*, **23**, 1223.
Cheng, A. Y. S., Hege, E. K., Hubbard, E. N., Goldberg, L., Strittmatter, P. A., and Cocke, W. J. 1986, *Ap. J.*, **309**, 737.
Clary, D. C. 1985, *Mol. Phys.*, **54**, 605.
Dalgarno, A., Oppenheimer, M., and Berry, R. S. 1973, *Ap. J.* (*Letters*), **183**, L21.
Deguchi, S. 1982, *Ap. J.*, **259**, 634.
Deguchi, S., and Goldsmith, P. F. 1985, *Nature*, **317**, 336.
Draine, B. T. 1978, *Ap. J. Suppl.*, **36**, 595.
Elitzur, M. 1980, *Ap. J.*, **240**, 553.
Forrest, W. J., McCarthy, J. F., and Houck, J. R. 1979, *Ap. J.*, **233**, 611.
Glassgold, A. E., and Huggins, P. J. 1986*a*, in *The M, S, and C Stars*, ed. H. R. Johnson and F. Querci (NASA/CNRS), in press.
———. 1986*b*, *Ap. J.*, **306**, 605.
Glassgold, A. E., Huggins, P. J., and Langer, W. D. 1985, *Ap. J.*, **290**, 615.
Glassgold, A. E., and Langer, W. D. 1974, *Ap. J.*, **193**, 73.
Glassgold, A. E., Lucas, R., and Omont, A. 1986, *Astr. Ap.*, **157**, 35 (Paper I).
Glassgold, A. E., Mamon, G. A., Omont, A., and Lucas, R. 1987, *Astr. Ap.*, **180**, 183 (Paper II).
Goldreich, P., and Scoville, N. Z. 1976, *Ap. J.*, **205**, 144 (GS).
Guilloteau, S., Lucas, R., Nguyen-Q-Rieu, and Omont, A. 1986, *Astr. Ap.*, **165**, L1.
Guilloteau, A., Omont, A., and Lucas, R. 1987, in preparation.
Hebden, J. C., Cheng, A. Y. S., Hege, E. K., Strittmatter, P. A., Beckers, J. M., and Murphy, H. P. 1986, *Ap. J.*, **309**, 745.
Hebden, J. C., Eckart, A., and Hege, E. K. 1987, *Ap. J.*, **314**, 690.
Herbst, E., and Klemperer, W. 1973, *Ap. J.*, **185**, 505.
Herbst, E., and Leung, C. M. 1986, *Ap. J.*, **310**, 378.
Herman, J. and Habing, H. J. 1985, *Phys. Rept.*, **124**, 255.
Herzberg, G. 1945, *Molecular Spectra and Molecular Structure. II. Infrared and Raman Spectra of Polyatomic Molecules* (New York: van Nostrand Reinhold), chap. 4.
Hollis, J. M., Churchill, E. B., Herbst, E., and de Lucia, F. C. 1986, *Nature*, **322**, 524.
Honeycutt, R. K., Bernat, A. P., Kephart, J. E., Gow, C. E., Sandford, M. T., and Lambert, D. L. 1980, *Ap. J.*, **239**, 565.
Hudson, R. D. 1971, *Rev. Geophys. Space Phys.*, **9**, 305.
Huggins, P. J., and Glassgold, A. E. 1982*a*, *A.J.*, **87**, 1828.
———. 1982*b*, *Ap. J.*, **252**, 201.
Jarrold, M. F., Bowers, M. T., DeFrees, D. J., McLean, A. D., and Herbst, E. 1986, *Ap. J.*, **303**, 392.
Jura, M. 1974, *Ap. J.*, **191**, 375.
Jura, M., and Morris, M. 1985, *Ap. J.*, **292**, 487.
Letzelter, C., Eidelsberg, M., Rostas, F., Breton, J., and Thieblemont, B. 1987, *Chem. Phys.*, in press.
Leung, C. M., Herbst, E., and Huebner, W. F. 1984, *Ap. J. Suppl.*, **56**, 231.
Liu, D.-J., and Oka, T. 1985, *Phys. Rev. Letters*, **54**, 1787.
Liu, D.-J., Oka, T., and Sears, T. J. 1985, *J. Chem. Phys.*, **84**, 312.
Lucas, R., Omont, A., Guilloteau, S., and Nguyen-Q-Rieu 1986, *Astr. Ap.*, **154**, L12.
Mamon, G. A., Glassgold, A. E., and Huggins, P. J. 1987, *Ap. J.*, submitted.
Mauron, N., Fort, B., Querci, F., Dreux, M., Fauconnier, T., and Lamp, P. 1984, *Astr. Ap.*, **130**, 341.
Millar, T. J., and Nejad, L. A. M. 1985, *M.N.R.A.S.*, **217**, 507.
Morris, M., and Alcock, C. 1977, *Ap. J.*, **218**, 687.
Morris, M., Guilloteau, S., Lucas, R., and Omont, A. 1987, preprint.
Morris, M., and Jura, M. 1983, *Ap. J.*, **264**, 546.
Mul, P. M., McGowan, J. W., Defrance, P., and Mitchell, J. B. A. 1983, *J. Phys. B*, **16**, 3099.
Nejad, L. A. M., Millar, T. J., and Freeman, A. 1984, *Astr. Ap.*, **134**, 129.
Nercessian, E., Forveille, T., Guilloteau, S., Lucas, R., and Omont, A. 1987, in preparation.
Omont, A. 1985, in *Mass-Loss from Red Giants*, ed. M. Morris and B. Zuckerman (Dordrecht: Reidel), p. 269.
Plummer, G. M., Herbst, E., and De Lucia, F. C. 1985, *J. Chem. Phys.*, **83**, 1428.
Scalo, J., and Slavsky, D. B. 1980, *Ap. J.* (*Letters*), **239**, L73.
Slavsky, D. B., and Scalo, J. 1984, preprint.
Smith, D., and Adams, N. G. 1984, *Ap. J.* (*Letters*), **284**, L13.
Sternberg, A., Dalgarno, A., and Lepp, S. 1987, preprint.
van Dishoeck, E. F. 1987, in *Astrochemistry*, ed. M. S. Vardya and S. P. Tarafder (Dordrecht: Reidel), p. 51.
van Dishoeck, E. F., and Dalgarno, A. 1984, *Ap. J.*, **277**, 576.
Walmsley, C. M. 1987, in *Astrochemistry*, ed. M. S. Vardya and S. P. Tarafder (Dordrecht: Reidel), p. 369.
Watson, W. D. 1973, *Ap. J.* (*Letters*), **183**, L17.
Wootten, A., Boulanger, F., Bogey, M., Combes, F., Encrenaz, P. J., Gerin, M., and Ziurys, L. 1986, *Astr. Ap.*, **166**, L15.

A. E. GLASSGOLD and G. A. MAMON: Department of Physics, New York University, 4 Washington Place, New York, NY 10003

A. OMONT: Groupe d'Astrophysique, Observatoire de Grenoble, CERMO, B.P. 68, 38402 Saint Martin d'Hères Cedex, France